Accepted Manuscript

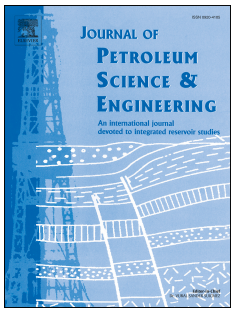

A new model for predicting fluid loss in nanoparticle modified drilling mud

Richard O. Afolabi

PII: S0920-4105(18)30725-3

DOI: 10.1016/j.petrol.2018.08.059

Reference: PETROL 5239

To appear in: *Journal of Petroleum Science and Engineering*

Received Date: 29 January 2018

Revised Date: 18 August 2018

Accepted Date: 20 August 2018

Please cite this article as: Afolabi, R.O., A new model for predicting fluid loss in nanoparticle modified drilling mud, *Journal of Petroleum Science and Engineering* (2018), doi: 10.1016/j.petrol.2018.08.059.

A New Model for Predicting Fluid Loss in Nanoparticle Modified Drilling Mud

Richard O. Afolabi

Department of Petroleum Engineering, Covenant University, P.M.B 1023, Ota, Nigeria.

Corresponding Author: richard.afolabi@covenantuniversity.edu.ng

Abstract

Attaining predictable properties for nano-modified drilling mud has evolved over time as a key challenge towards its application. The known predictive models used in the description of drilling mud performance cannot quantitatively capture the impact of nanoparticles. In this work, existing theories on the kinetics of mud cake formation and colloidal particle behavior were applied in deriving a new fluid loss model. The new model described the fluid loss behavior of the mud with the capability of predicting a maximum for cumulative value. The new model was compared with the known API model using statistical measures, Root Mean Square Error (RMSE) and Coefficient of Determination (R^2). The new model compares favorably with the API model with RMSE and R^2 values 0.8549 - 0.4595 cm^3 and 98.9 - 99.9 % respectively. The development of the model for nano-drilling fluids would allow for detailed modeling, design and cost-effective drilling operations as the quantitative amount of nanoparticles required would be captured.

Keywords: Nanotechnology; Bentonite Muds; Filtration; Predictive Modelling

Highlights

- Kinetics of mud cake formation and colloidal behavior used for fluid loss model.
- The new fluid loss model was able to predict a value for the maximum fluid loss.
- The new model captured the quantitative amount of nanoparticles required.

1. Introduction

Drilling muds are required to perform multiple tasks concurrently in the drilling environment while maintaining the required hydrostatic head (Zheng and Ma, 2010; Sadeghalvaad and Sabbaghi, 2015; Mahmoud et al., 2016; Ismail et al., 2016; Vryzas and Kelessidis, 2017). The need for an efficient drilling mud systems has brought about increased research channeled towards improving mud performance in tough drilling conditions (Kelessidis and Maglione, 2008; Abu-Jdayil, 2011; Lee et al., 2012; Fazelabdolabadi et al., 2015). Nanotechnology has been at the forefront over the past couple years as a key area of research towards improving the properties of drilling fluids (Abdo and Danish-Haneef, 2012; Hoelscher et al., 2012; Ismail et al., 2016). It is projected that the use of nanoparticles will play an important role in the production of drilling fluids, which can stand tough drilling environments (Vryzas and Kelessidis, 2017). A key challenge identified by the application of nano-drilling muds is the quantitative computation of the impact of nanoparticles (Vryzas and Kelessidis, 2017). The work of Reilly et al. (2016) and Gerogiorgis et al. (2017) laid a good foundation for the development of rheological models, which captures the quantitative contribution of nanoparticles to the overall rheology of drilling fluids. Furthermore, extending the work to cover other aspects of drilling mud performance such as fluid loss behavior is required. The development of models for describing the fluid behavior of nanoparticle-enhanced drilling fluids is critical towards successful modeling, design and cost-effective drilling operations involving nanoparticles (Vryzas and Kelessidis, 2017). It is against this background that this study applied existing theories on the kinetics of mud cake formation and colloidal particle behavior was applied in deriving a new fluid loss model, which describes the fluid loss of nanoparticle-enhanced water-based mud. This was done taking into account the kinetics of mud cake formation and colloidal behavior of the nanoparticles as described by Reilly et al. (2016) and Gerogiorgis et al. (2017). The new model captured the quantitative contribution of

nanoparticles to the fluid loss of water-based mud in terms of the size of the nanoparticles, quantity of nanoparticles and the type of nanoparticles. This is significant in computational modeling of the effect of changes in size, and concentration of nanoparticles, which can be related explicitly to fluid loss.

2. Development of Fluid Loss Model

2.1 Kinetics of Mud Cake Formation during Filtration

A non-dimensional parameter is used in describing the changes in the concentration of clay particles in a bentonite suspension. The concentration of clay particles, C, is used as a measure of the amount of clay particles in the bentonite suspension at any given time. The non-dimensional parameter, ζ, is related to the concentration of clay particles at any given time and initial concentration of clay particles, C_o using a similar approach by (Toorman, 1997)

$$\zeta = \frac{C}{C_o} \tag{1}$$

$$C = C_o \ (\zeta = 1) \tag{2}$$

The rate of diffusion of clay particles to the surface of a mud cake depends on the difference between the maximum concentration of clay particles in the drilling mud, ζ_0 (value of 1) and the concentration of clay particles at any given point in time, ζ. Hence, the rate of diffusion of clay particles is expressed as

$$\frac{d\zeta_r}{dt} = a(\zeta_0 - \zeta)^m \tag{3}$$

where a is the diffusion parameter and m is the diffusion exponent The rate of clay particle build-up on the mud cake is dependent on the time of consolidation of particles on the mud cake, t, and concentration of clay particles in the bentonite suspension at any point in time, ζ. The rate of build-up is expressed as

$$\frac{d\zeta_b}{dt} = bt\,\zeta^{n_b} \quad (4)$$

where b is the build-up constant and n_b is the build-up exponent. The net rate expression is the difference between the rate of diffusion and that of build-up.

$$\frac{d\zeta}{dt} = a(\zeta_0 - \zeta)^m - bt\,\zeta^{n_b} \quad (5)$$

Assuming a first-order rate kinetics for the diffusion and build-up expressions, $m = n_b = 1$.

$$\frac{d\zeta}{dt} = a(\zeta_0 - \zeta) - bt\zeta \quad (6)$$

At equilibrium, the rate of diffusion equals the rate of build-up. Therefore, $\frac{d\zeta}{dt} = 0$

$$a(\zeta_0 - \zeta_e) = bt\,\zeta_e \quad (7)$$

$$\zeta_e = \frac{1}{1+\beta t} \quad (8)$$

where β is the ratio of the build-up constant b to the diffusion parameter a.

2.2 Colloidal Behaviour of Nanoparticles

The theory of colloidal particle behavior in bentonite suspension follows the description of (Gerogiorgis et al., 2017). The distribution and arrangement of nanoparticles in the suspension was assumed to follow a cubical arrangement with an explicit expression as shown in (9)

$$h_{np} = 4r_{np} + r_{np}\sqrt[3]{\frac{4\pi}{3\emptyset}} \quad (9)$$

h_{np} is the inter-particle distance between nanoparticles, r_{np} is the radius of nanoparticles and $\emptyset$ is the fractional volume of nanoparticles (Gerogiorgis et al., 2017). Inserting equation (8), equation (9) becomes

$$h_{np} = 4r_{np}\left(\frac{1}{1+\beta t}\right) + \left(1 - \frac{1}{1+\beta t}\right) r_{np} \sqrt[3]{\frac{4\pi}{3\emptyset}} \quad (10)$$

Equation (10) is similar to the shear-dependent inter-particle distance derived by (Gerogiorgis et al., 2017).

2.3 Fluid Loss Model

A general equation describing the fluid loss (V_f) behaviour of a nano-drilling mud combines the fluid loss due to the clay particles, V_{cp}, and the fluid loss attributable to the presence of nanoparticles, V_{np}.

$$V_f = V_{cp} + V_{np} \quad (11)$$

According to Darley and Gray (1988), the API model for predicting the fluid loss due to clay particles is represented in (12)

$$V_f^2 = \frac{2kPA^2}{\mu}\left(\frac{V_f}{V_c}\right) t = V_f = \alpha\sqrt{t} \quad (12)$$

Where $\alpha = \sqrt{\frac{2kPA^2}{\mu}\left(\frac{V_f}{V_c}\right)}$. For a given suspension, $\frac{V_f}{V_c}$ and k in (12) is constant with respect to time (Darley and Gray, 1988). According to Vipulanandan et al. (2014), the permeability of a mud cake, k and the ratio $\frac{V_f}{V_c}$ are both functions of time. In order to account for the time variation of $\frac{V_f}{V_c}$ and k, equations (13) and (14) are introduced as follows using the approach of Vipulanandan et al. (2014):

$$\frac{V_f}{V_c} = f(\zeta_e, t) = \frac{1}{1+\beta t} t \quad (13)$$

$$k = f(\zeta_e, k_o) = \frac{1}{1+\beta t} k_o \quad (14)$$

k_o is the initial permeability of the formed mud cake. Substituting (13) and (14) into (12), yields

$$V_f = V_{cp} = \left[\sqrt[2]{\left(\frac{2Pk_o}{\mu}\right)}\right] A \left[\frac{t}{1+\beta t}\right] \quad (15)$$

Continuous deposition of solids from the drilling mud to the formed mud cake means that the inter-particle distance changes with filtration time. As solids decrease in the drilling mud, the distance between the particles increases. According to Gerogiorgis et al. (2017), the van der Waals force of attraction between nanoparticles during the filtration process becomes

$$F_{VDW} = \frac{Ar_{np}}{12h_{np}^2} \quad (16)$$

A is the Hamaker constant. Substituting the expression derived in (10) for h_{np} into (16)

$$F_{VDW} = \frac{Ar_{np}}{12\left[4r_{np}\left(\frac{1}{1+\beta t}\right)+\left(1-\frac{1}{1+\beta t}\right)r_{np}\sqrt[3]{\frac{4\pi}{3\emptyset}}\right]^2} \quad (17)$$

Under static filtration conditions, the hydrostatic pressure acting on the column of fluid is given as described by (Nihous, 2016)

$$P_{hyd} = \rho_f g h \quad (18)$$

The normal force due to the hydrostatic pressure acting on the nanoparticles is given in (19)

$$F_{norm} = \rho_f g A h \quad (19)$$

$$F_{norm} = V_{np} \rho_f g \quad (20)$$

where F_{norm} is the normal force due to hydrostatic pressure, V_{np} is the fluid loss due to the presence of nanoparticles, ρ_f is the density of the fluid and g is the acceleration due to

gravity. Equating the normal force, F_{norm} in (20) to the expression for Van der Waals force, F_{VDW} in (17) and simplifying,

$$V_{np} = \frac{Ar_{np}}{12\rho_f g\left[4r_{np}\left(\frac{1}{1+\beta t}\right)+\left(1-\frac{1}{1+\beta t}\right)r_{np}\sqrt[3]{\frac{4\pi}{3\emptyset}}\right]^2} \quad (21)$$

The fluid loss model incorporating the contribution of nanoparticles is obtained by adding equation (21) to equation (15) as represented in (11).

$$V_f = N\left[\frac{t}{1+\beta t}\right] + \left[\frac{Ar_{np}}{12\rho_f g\left[4r_{np}\left(\frac{1}{1+\beta t}\right)+\left(1-\frac{1}{1+\beta t}\right)r_{np}\sqrt[3]{\frac{4\pi}{3\emptyset}}\right]^2}\right] \quad (22)$$

Equation (22) represents a new fluid loss model accounting for the variation of solids on the mud cake, variation of the mud cake permeability and the effect of nanoparticles on the fluid loss. The maximum fluid loss prediction becomes

$$\lim_{t\to\infty} V_f = \frac{N}{\beta} + \frac{Ar_{np}}{12\rho_f g\left[r_{np}\sqrt[3]{\frac{4\pi}{3\emptyset}}\right]^2} \quad (23)$$

The impact of nanoparticles on the maximum fluid loss is quantitatively captured in equation (24). This is reflected in terms of the size of the nanoparticles, quantity of nanoparticles and the type of nanoparticles.

3. Materials and Method

3.1 Materials

3.1.1 Bentonite Clay

The natural bentonite clay was acquired from a local supplier in Nigeria. The clay storage condition in the laboratory was between 27°C to 30°C. The mineralogical analysis was carried out using the PAN Analytical X-Pert Pro diffractometer operating at 30 kV and 40

mA. The mineral composition is contained in Table 1. Investigation of the elemental composition of the bentonite clay was done using Energy Dispersive X-Ray (EDX) spectroscopy. This was carried out using the Phenom® ProX desktop Energy Dispersive X-Ray (EDX) machine as reported in Table 2. Particles size distribution of the bentonite clay was measured using a laser scattering particle size analyzer (Shimadzu® Particle Size Analyzer). The average particle size for the bentonite clay is 4 μm (Figure 1).

3.1.2 Silica Nanoparticles

Silica (SiO_2) nanoparticles were also acquired from a local supplier in Nigeria. The nanoparticles were manufactured by Sigma Aldrich and have the following physical properties; appearance: white powder, size: 50 ± 4 nm (TEM), purity: 99.8 %, surface area (BET): 60.2 m^2/g.

3.2 Preparation of Drilling Mud

Nanofluids were prepared by adding 4, 6, 8 g of silica nanoparticles in 350 mL of distilled water. The dispersed nanoparticles were stirred using a Hamilton beach mixer at a speed of 11000-RPM until silica nanofluids were obtained. These nanofluids act as the base fluids for the preparation of the drilling mud. 25 g of the bentonite clay was added to each of the prepared nanofluids and stirred for 20 minutes after which the nanoparticle enhanced water-based drilling mud was obtained.

3.3 Fluid Loss Determination

The experimental procedure for the fluid loss determination was carried out in accordance with the API Specification 13-A for drilling fluid materials. The nano-modified water-based mud was filtered through the OFITE Low-Pressure Low Temperature (LPLT) filter press at 100 psi and 25 ^0C for low-pressure low-temperature conditions. A timer was set for 30 minutes with the fluid loss collected at every 5-minute interval.

4. Results and Discussion

4.1. Impact of Silica Nanoparticles on Fluid Loss of Drilling Mud

The effect of silica nanoparticles on the mud cake can be established to reduce the permeability of the drilling mud cake thereby reducing the fluid loss volume. The high surface area and small size of nanoparticles enable them to form fine dispersions and tight packing structures thereby effectively filling *"fluid flow"* gaps that exist between micron-size particles. This phenomenon also applies to the mud cake, which is formed during the static filtration process involving nano-modified drilling fluids. This reduces the mud cake permeability and subsequently fluid loss. The reduction in mud cake permeability by the silica nanoparticles is due to the plugging capability of the nanoparticles on the mud cake thereby producing a low permeability medium. The works of (Ragab and Noah, 2014; Yang et al., 2015; Ghanbari et al., 2016) have confirmed the plugging capabilities of nanoparticles in rock formations. The significance of mud cake permeability reduction is critical towards successful drilling operations. Since the differential force acting on a drill pipe increases from the time of initial contact until leak-off of the filtrate from the cake has allowed complete development of the differential pressure, some incidents of sticking may be eliminated if the rate of application of the differential force can be slowed. The rate of increase of the differential force is a function of the rate of flow of filtrate out of the cake. This can be controlled by the cake permeability and thickness. Decreasing the permeability and thickness of the cake using nanoparticles would increase the time required to stick the pipe.

4.2. Cumulative Fluid Loss Prediction

The cumulative fluid loss prediction was done using the new fluid loss model in equation (23). This was fitted to the experimental fluid loss data obtained and comparison made with the API model. Experimental fluid loss data from four samples containing 4 g (S_1), 6 g (S_2) and 8 g (S_3), of silica nanoparticles dispersed in 25 g bentonite mud were used for the model

fitting. The model fitting for sample S_2 showed a coefficient of determination value of 0.984 for the API model while the new fluid loss model was 0.995. Based on the RMSE, the values obtained were 3.4251 and 2.0255 cm^3 for the API and new models respectively. The new model seems to be the better fit when using the statistical measures. Samples S_1 and S_3 gave the coefficient of determination values of 0.999 and 0.999 for the new model and 0.996 and 0.989 for the API model respectively. The RMSE values were 0.8549 and 0.4595 cm^3 for the new model and 1.7697 and 2.6231 cm^3 for the API model respectively. The new fluid loss model gave a better prediction for samples S_2 and S_3 based on the statistical measures. Plots of the fitted models (API and New Model) to the experimental fluid loss data for the various samples are shown in Figures 2 – 4. Comparison between the API model and the new model was also done based on the confidence interval. Figures 5 – 7 show the 95% confidence interval for samples 1 – 3 using the API and new models. The narrow confidence interval associated with the new model for samples 1 – 3 is indicative of the precision of the model in predicting the response for a specified set of the predictor variable. The wide confidence interval associated with the API model in Figures 5 – 7 imply that there is less confidence in the precision of the model for the prediction of future values of the cumulative fluid loss. The new fluid loss model gave a better description of the fluid loss behavior of the nano-drilling mud. This could be explained in terms of the approach used in the derivation of the new fluid loss model. The kinetics of the mud cake formation from the deposition of clay particles and the colloidal behavior of nanoparticles were employed. The API model employs a generalized approach in describing the fluid loss of nano-drilling muds. The API model does not capture the quantitative contribution of nanoparticles to fluid loss. The standard error (SE) of the model parameters for the API and new models are contained in Table 3 respectively. For the new model, r_{np}, A, and $\emptyset$ represent material properties associated with the nanoparticles. They are not estimated through regression analysis, rather are material

constants determined based on the physical properties of the nanoparticles. For samples 1, 2, and 3, the SE values for the parameters associated with the new model are smaller compared to the API model. This shows the precision of the values estimated for the parameters of the new model. In addition, the lower values for the margin of error associated with the confidence interval also indicates the precision of the parameter estimates. For sample 3, the margin of error for the parameters of the new model (N and β) are 0.19 and 0.01 respectively. For the API model, the margin of error for the parameter α is 0.624. The precision of the parameters associated with the new model are higher compared with the API model.

5. Conclusion

A basic foundational approach was applied in deriving a novel model, which describes the impact of the nanoparticles on the fluid loss of drilling mud during the filtration process. This was done taking into account the kinetics of mud cake formation and colloidal behavior of the nanoparticles. The new model gave a better description of the fluid loss behavior of the nano-drilling mud when compared with the API model using statistical measures. This is due to the following:

a) The development of the new model accounted for mud cake permeability variation with filtration time
b) The new model development also considered the variation of solid fraction with filtration time

The new model also captured the quantitative contribution of nanoparticles to the fluid loss of water-based mud in terms of the size of the nanoparticles, quantity of nanoparticles and the type of nanoparticles. This is significant in computational modeling of the effect of changes in size, and concentration of nanoparticles, which can be related explicitly to fluid loss.

Accurate prediction of the quantitative amount of nanoparticles required for a particular fluid loss reduction would enable cost-effective planning of drilling operations. Ongoing research by the author involves modifying the proposed model to incorporate temperature effects. This would ensure accurate description of the explicit effect of temperature conditions on the fluid loss reduction by nanoparticles. Further research is still required in developing models, which describes the effect of nanoparticles on:

c) The mud cake permeability with filtration time

d) The thickness of mud cake with filtration time

Acknowledgment

The author, for providing an enabling environment to carry out this research, appreciate the management of Covenant University.

Nomenclature

C_o	Initial Concentration or Volume Fraction of Clay Particles (dimensionless)
C	Concentration or Volume Fraction of Clay Particles at Time t (dimensionless)
g	Acceleration due to Gravity, cm/s^2
ρ_f	The Density of Fluid, g/cm^3
ϕ	Volume Fraction of Nanoparticles (dimensionless)
r_{np}	The Radius of Nanoparticles, nm
A	Hamaker Coefficient or Constant, J
A_c	Area of Mud Cake, cm^2
k_o	Initial Permeability of Mud Cake, mD

k	Permeability of Mud Cake, mD
A_{np}	Area of Nanoparticles, cm^2
h	Mud Cake Thickness, cm
h_{np}	Inter-particle Distance between Nanoparticles, m
V_{np}	The Volume of Nanoparticles, cm^3
V_f	The Volume of Fluid, cm^3
V_c	The Volume of Mud Cake, cm^3
ζ	Non-dimensional Parameter at any Time
ζ_o	Non-dimensional Parameter at C_o
ζ_e	Equilibrium Parameter (dimensionless)
ζ_b	Non-dimensional Parameter for Build-Up
ζ_r	Non-dimensional Parameter for rate of diffusion
F_{VDW}	Van Der Waals Force of Attraction, N
F_{norm}	Normal Force due to Hydrostatic Pressure, N
V_{disp}	Volume due to Displacement of Fluid, cm^3
m	Diffusion Exponent (dimensionless)
a	Diffusion Parameter (dimensionless)
b	Build-up Constant (dimensionless)
t	Time, mins

β	Ratio of Build-up Constant to Diffusion Parameter (dimensionless)
n_b	Build-up Exponent (dimensionless)

Funding

A specific grant from funding agencies in the public, commercial, or not-for-profit sectors was not received for this research work.

Conflict of Interest

The author has no conflict of interest to declare.

References

Abdo, J., & Danish-Haneef, M. (2012). Nano-Enhanced Drilling Fluids: Pioneering Approach to Overcome Uncompromising Drilling Problems. *Journal of Energy Resources Technology*, *134*: 1-6.

Abu-Jdayil, B. (2011). Rheology of Sodium and Calcium Bentonite-Water Dispersions: Effect of Electrolytes and Aging Time. *International Journal of Mineral Processing*, *98*: 208-213

Darley, H. C., & Gray, G. R. (1988). Composition and Properties of Drilling and Completion Fluids (5th ed.). Houston-Texas: Gulf Professional Publishing.

Fazelabdolabadi, B., Khodadadi, A. A., & Sedaghatzadeh, M. (2015). Thermal And Rheological Properties Improvement of Drilling Fluids using Functionalized Carbon Nanotubes. *Applied Nanoscience*, *5*: 651-659.

Gerogiorgis, D. I., Reilly, S., Vryzas, Z., & Kelessidis, V. C. (2017). Experimentally Validated First-Principles Multivariate Modelling for Rheological Study and Design of

Complex Drilling Nanofluid Systems. *SPE/IADC Drilling Conference and Exhibition* (pp. 1-11). Hague: Society of Petroleum Engineers.

Ghanbari, S., Kazemzadeh, E., Soleymani, M., & Naderifar, A. (2016). A Facile Method for Synthesis and Dispersion of Silica Nanoparticles in Water-Based Drilling Fluid. *Colloid and Polymer Science*, 294(2): 381-388.

Hoelscher, K. P., Stefano, G., Riley, M., & Young, S. (2012). Application of Nanotechnology in Drilling Fluids. *SPE International Oilfield Nanotechnology Conference* (pp. 1-7). Noordwijk: Society of Petroleum Engineers.

Ismail, A. R., Aftab, A., Ibupoto, Z. H., & Zolkifile, N. (2016). The Novel Approach for the Enhancement of Rheological Properties of Water-Based Drilling Fluids using Multi-Walled Carbon Nanotubes, Nanosilica, and Glass Beads. *Journal of Petroleum Science and Engineering*, *139*: 264-275.

Kelessidis, V. C., & Maglione, R. (2008). Yield Stress of Water-Bentonite Dispersions. *Colloids and Surfaces A: Physiochemical and Engineering Aspects*, *318*: 217-226.

Lee, E. J., Stefanus, C., & Leong, Y. K. (2012). Structural Recovery Behaviour of Kaolin, Bentonite and K-Montmorillonite Slurries. *Powder Technology*, *223*: 105-109.

Mahmoud, O., Nasr El-Din, H., Vryzas, Z., & Kelessidis, V. (2016). Nanoparticle-Based Drilling Fluids for Minimizing Formation Damage in HP/HT Applications. *SPE International Conference and Exhibition on Formation Damage and Control* (pp. 1-26). Louisiana: Society of Petroleum Engineers.

Nihous, G. C. (2016). Notes on Hydrostatic Pressure. Journal of Ocean Engineering and Marine Energy, 2(1), 105-109.

Ragab, A. M., & Noah, A. (2014). Reduction of Formation Damage and Fluid Loss using Nano-Sized Silica Drilling Fluids. *Petroleum Technology Development Journal*, 2: 75-88.

Reilly, S., Vryzas, Z., Kelessidis, V. C., & Gerogiorgis, D. I. (2016). First Principles Rheological Modelling and Parameter Estimation for Nanoparticle-Based Smart Drilling Fluids. *European Symposium on Computer Aided Process Engineering* (pp. 1-6). Portoroz: Elsevier B. V.

Sadeghalvaad, M., & Sabbaghi, S. (2015). The Effect of the TiO_2/Polyacrylamide Nanocomposite on Water-Based Drilling Fluid Properties. *Powder Technology*, *272*: 113-119

Toorman, E. A. (1997). Modelling the thixotropic behaviour of dense cohesive sediment suspensions. *Rheologica Acta*, *36*(1): 56-65.

Vipulanandan, C., Raheem, A., Basirat, B., & Mohammed, A. S. (2014). New Kinetic Model to Characterise the Filter Cake Formation and Fluid Loss in HPHT Process. *Offshore Technology Conference* (pp. 1-17). Houston-Texas: Society of Petroleum Engineers.

Vryzas, Z., & Kelessidis, V. C. (2017). Nano-Based Drilling Fluids: A Review. *Energies*, *10*: 1-34.

Yang, X., Yue, Y., Cai, J., Liu, Y., & Wu, X. (2015). Experimental Study and Stabilization Mechanisms of Silica Nanoparticles Based Brine Mud with High-Temperature Resistance for Horizontal Shale Gas Wells. *Journal of Nanomaterials*, 1-10.

Zheng, X., & Ma, X. (2010). *Drilling Fluids*. Beijing: China University of Geosciences

Table 1: Mineralogical composition of the bentonite clay

Mineral	Montmorillonite	Kaolinite	Quartz	Calcite	Feldspar	Biotite
% Composition	22.19	4.91	42.91	12.98	13.78	3.23

Table 2: Compositional analysis of the bentonite clay showing the various oxides present in the clay sample.

Element	**SiO_2**	**Al_2O_3**	**Fe_2O_3**	**Na_2O**	**CaO**	**K_2O**	**MgO**	**TiO_2**	**LOI**
%	55.33	25.69	3.86	4.4	2.65	1.7	2.3	1.1	2.97

Table 3: Parameter estimation and confidence interval for the API and New models respectively.

Sample	*Model	Parameter	Estimate	Standard Error of Estimate (SE)	95% Confidence Interval
1	API	α	9.82	0.173	9.401 - 10.25
	New	N	5.13	0.141	4.564 - 5.799
		β	0.06	0.005	0.052 - 0.079
2	API	α	8.32	0.334	7.506 - 9.141
	New	N	2.69	0.296	2.025 - 3.692
		β	0.02	0.007	0.006 - 0.046
3	API	α	7.31	0.256	6.686 - 7.938
	New	N	2.54	0.074	2.353 - 2.738
		β	0.03	0.002	0.021 - 0.032

** For the new model, r_{np}, A, and $\emptyset$ represent material properties associated with the nanoparticles. They are not estimated through regression analysis, rather are material constants.*

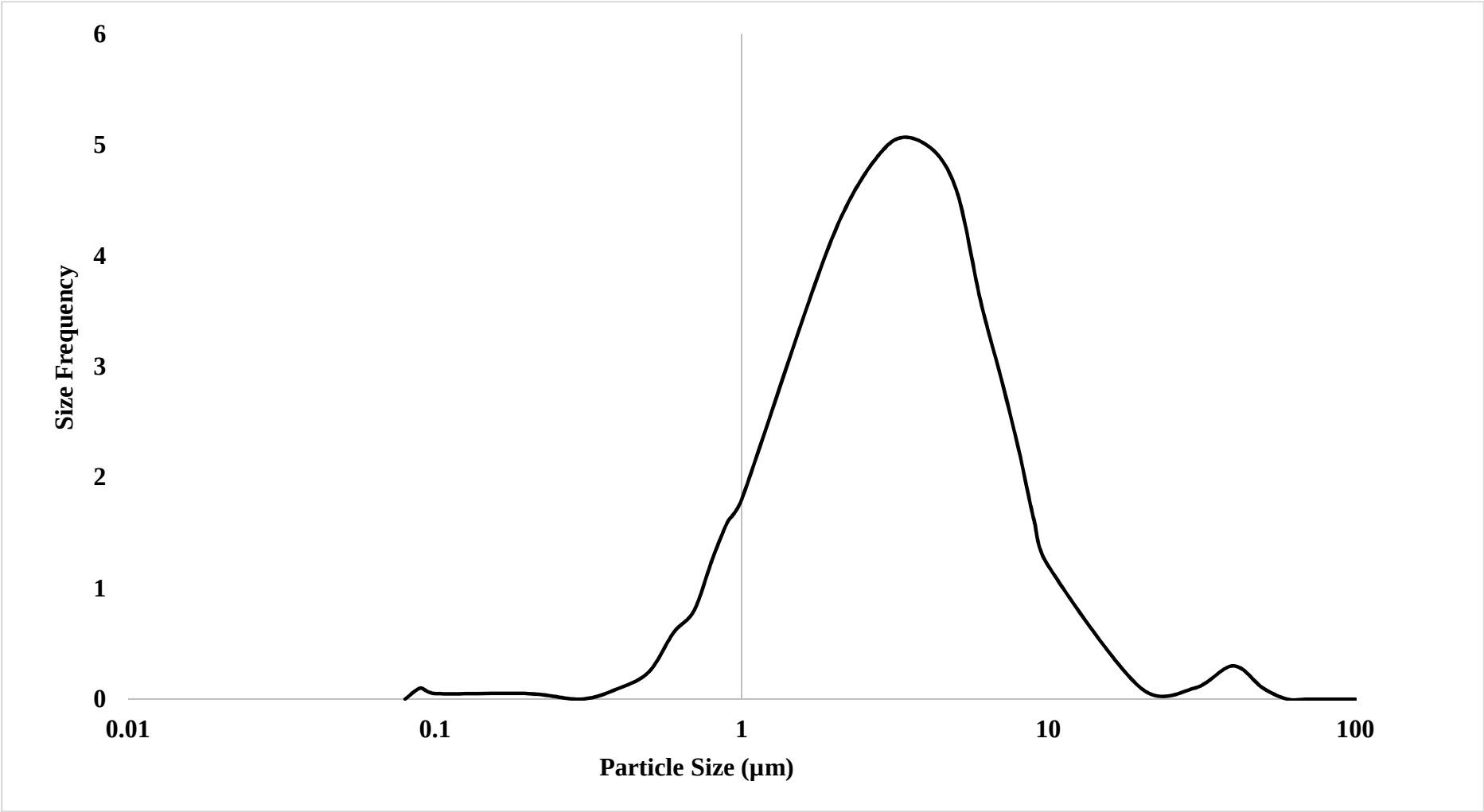

Figure 1: Particle size distribution for the bentonite clay

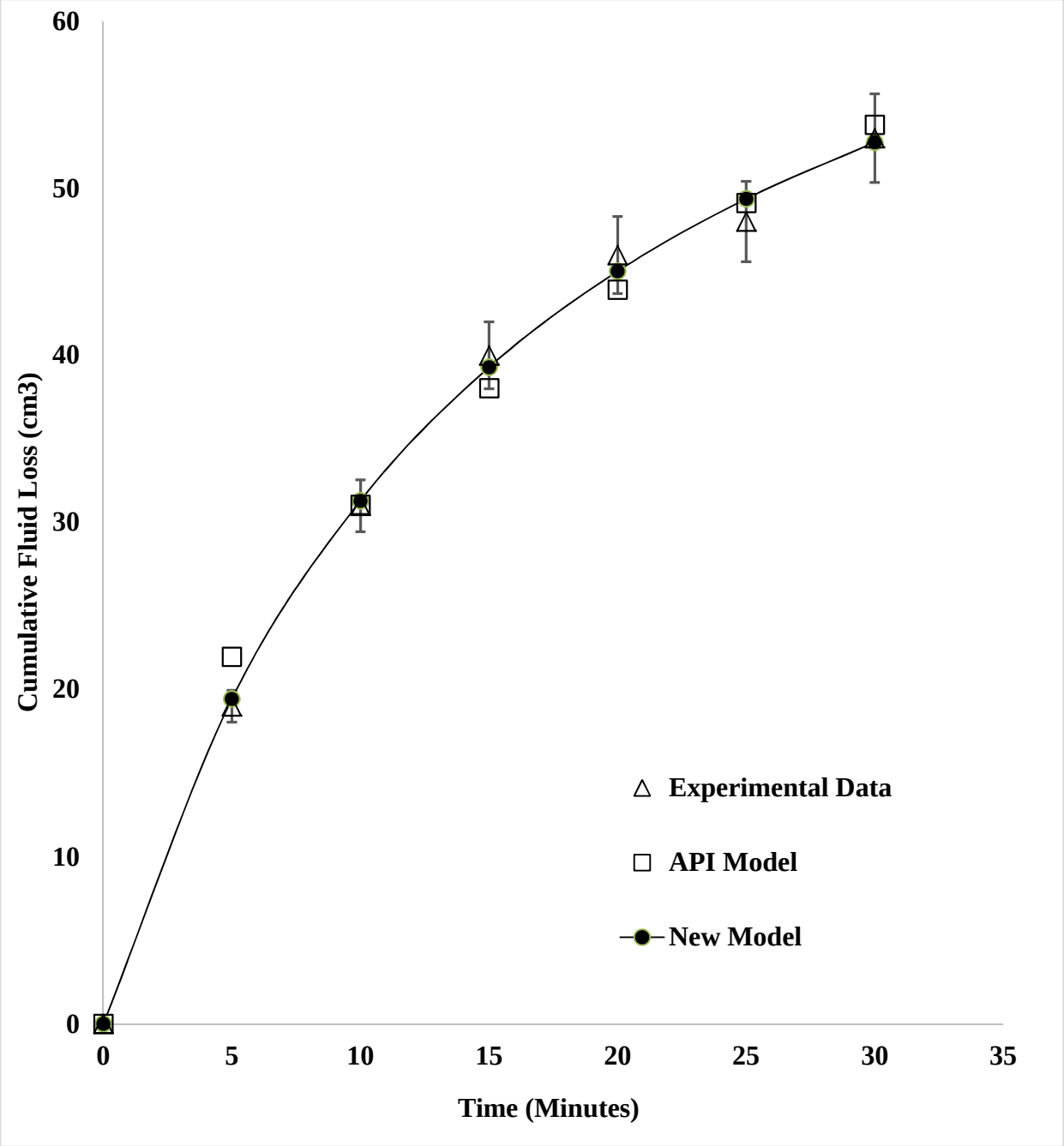

Figure 2: Cumulative fluid loss prediction using API and new fluid loss model for mud sample S_1 containing 4 g silica nanoparticles and 25 g bentonite at 25 ^0C and 100 psi

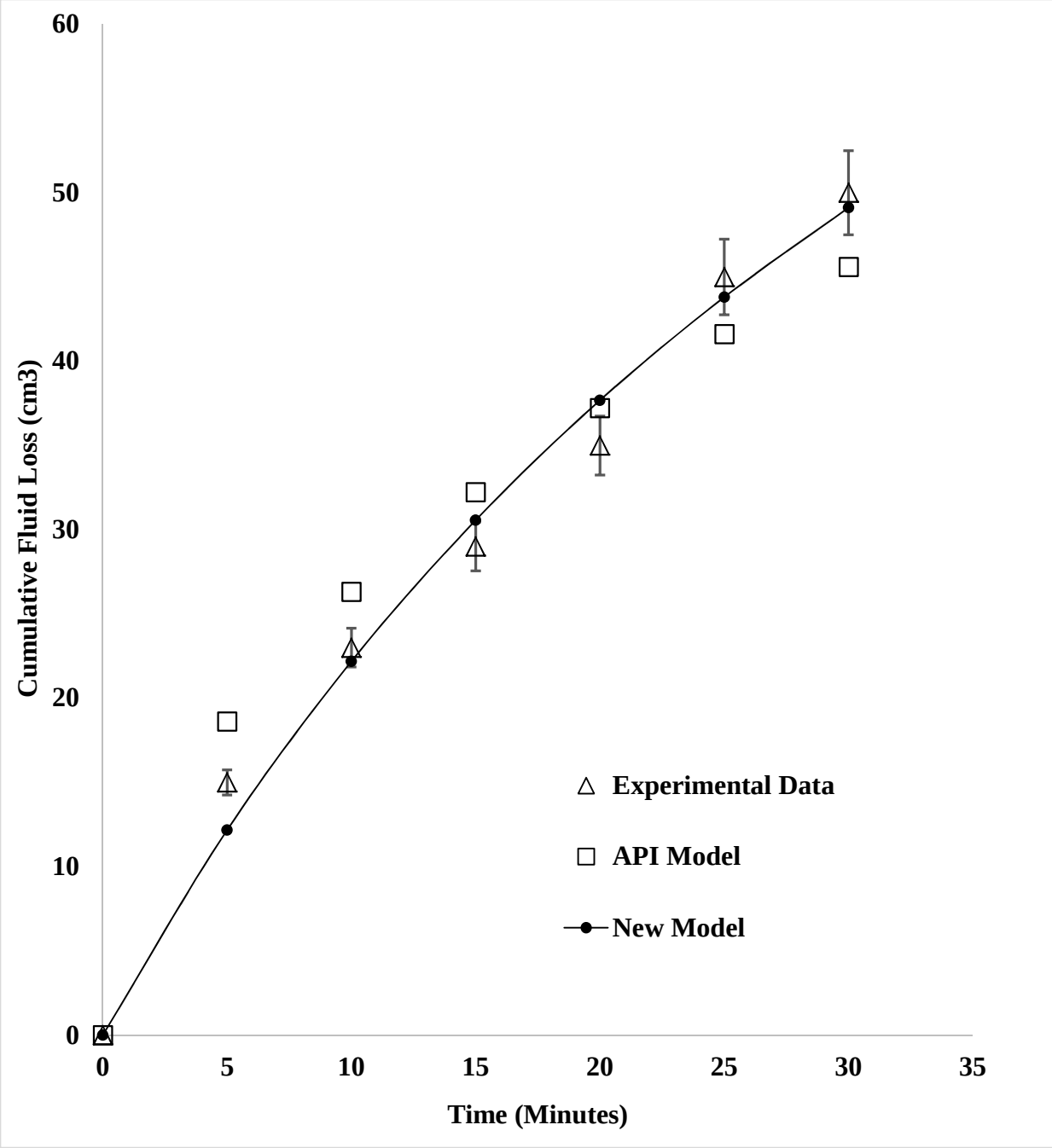

Figure 3: Cumulative fluid loss prediction using API and new fluid loss model for mud sample S_2 containing 6 g silica nanoparticles and 25 g bentonite at 25 ^{0}C and 100 psi.

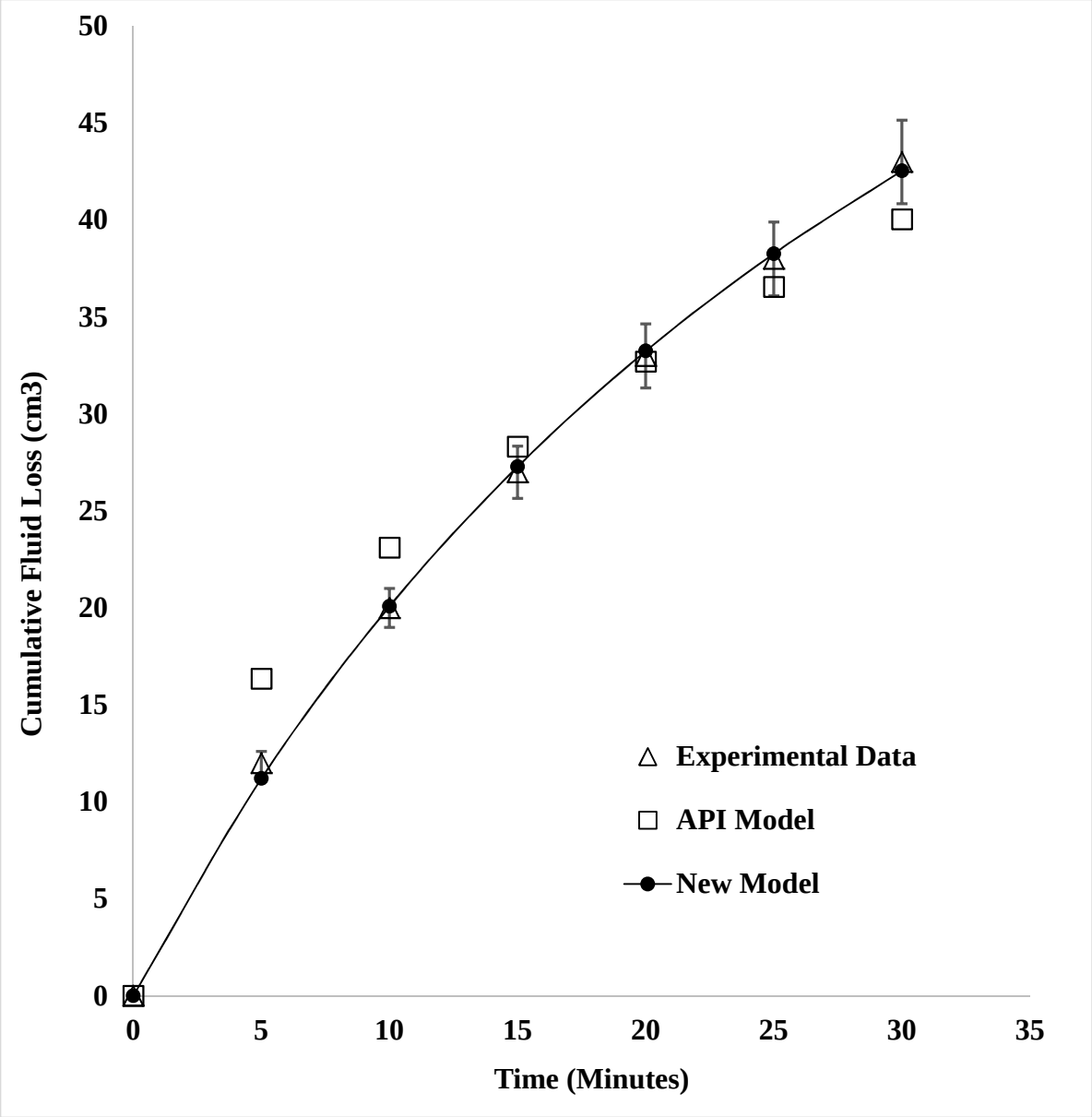

Figure 4: Cumulative fluid loss prediction using API and new fluid loss model for mud sample S_3 containing 8 g silica nanoparticles and 25 g bentonite at 25 ^{0}C and 100 psi.

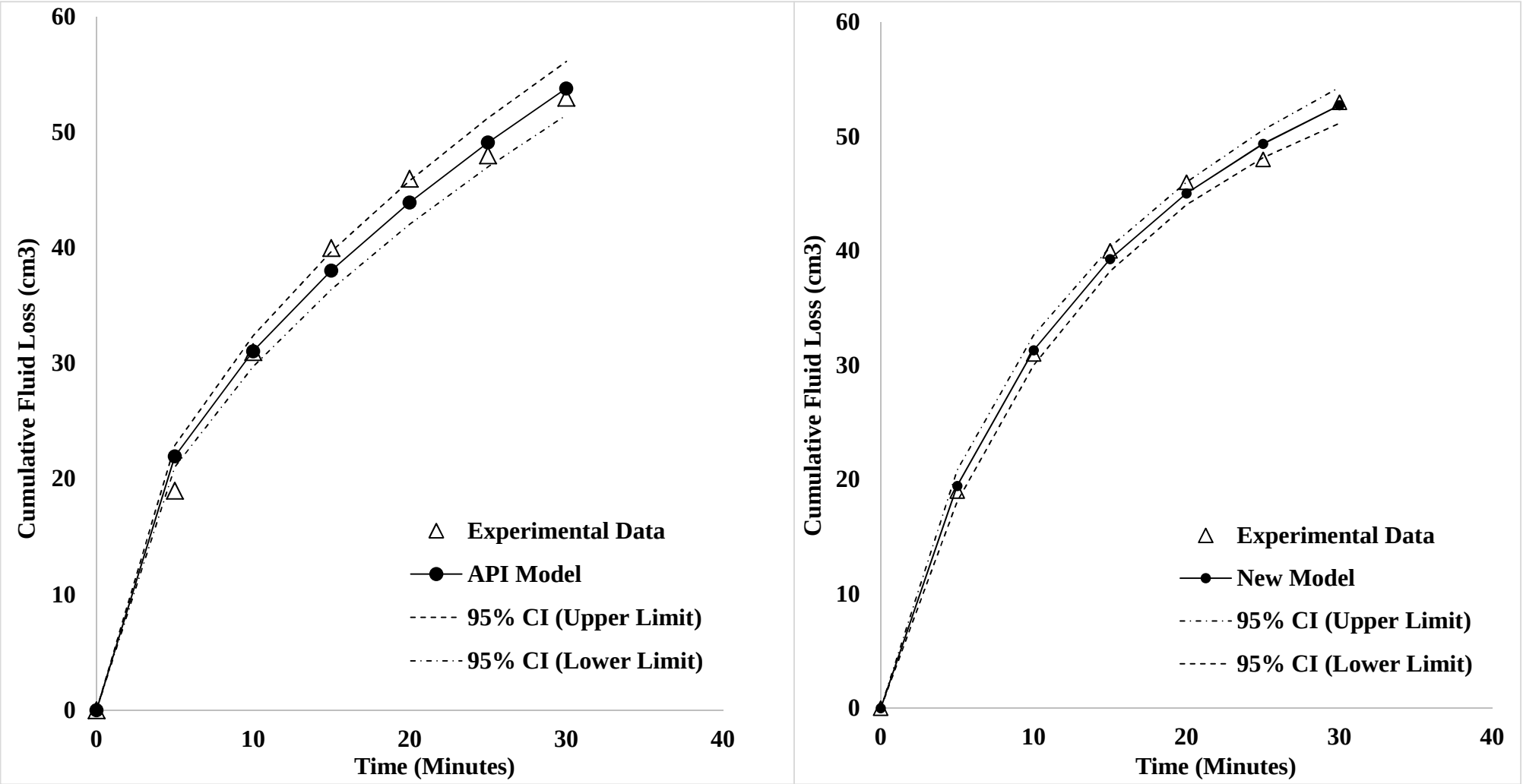

Figure 5: The prediction for Sample 1 at 95% confidence interval for (a) API model and, (b) New model

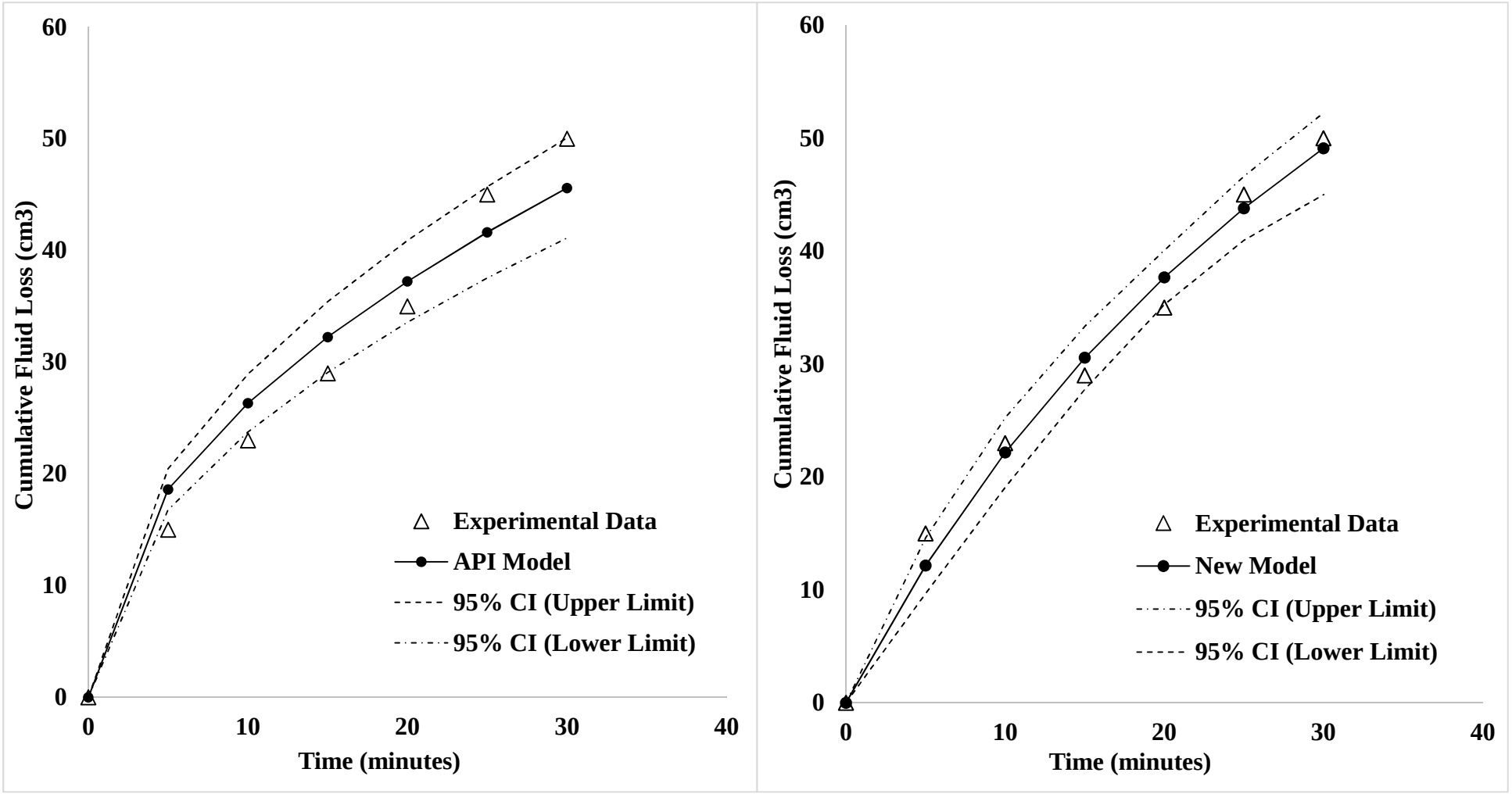

Figure 6: The prediction for Sample 2 at 95% confidence interval for (a) API model and, (b) New model

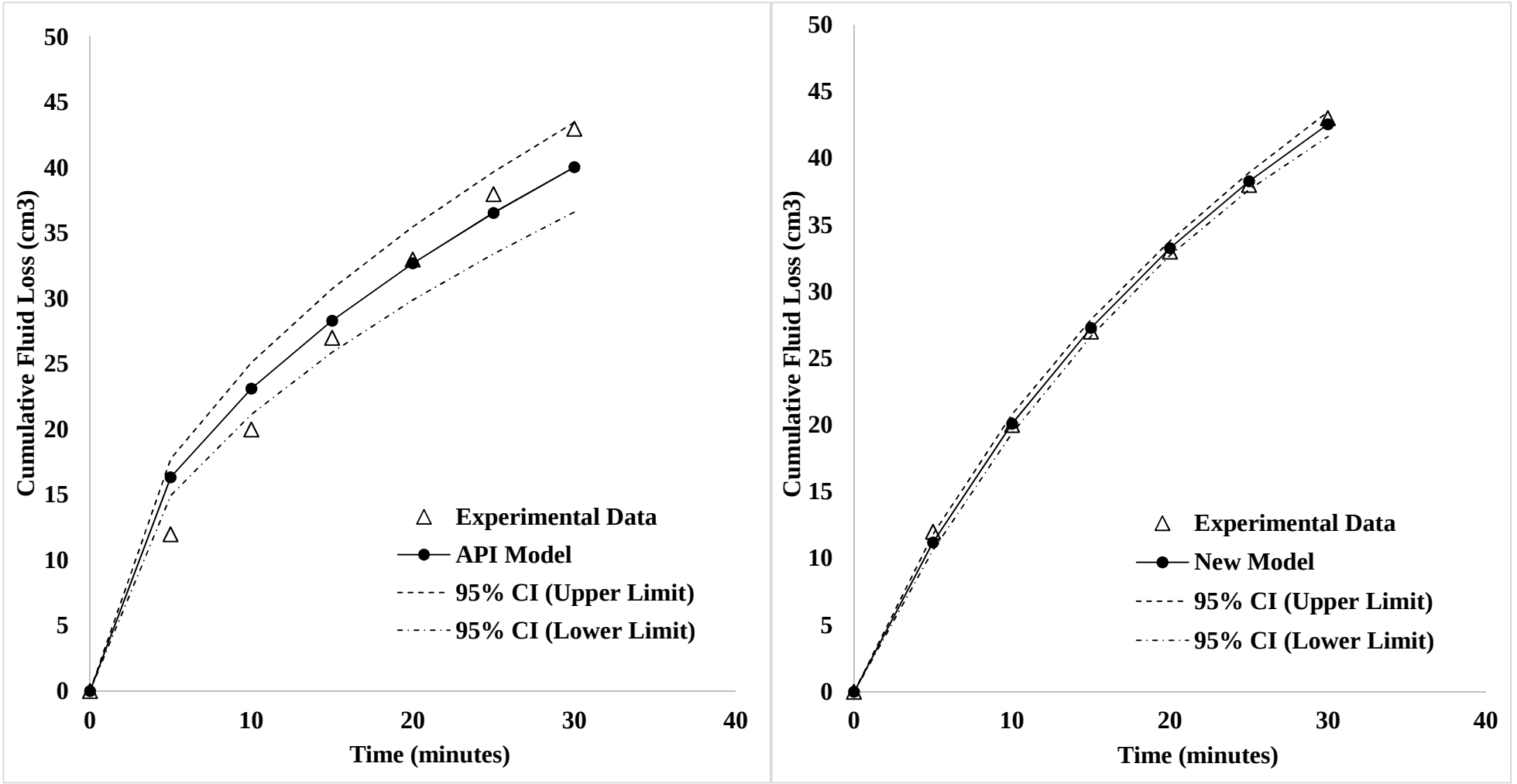

Figure 7: The prediction for Sample 3 at 95% confidence interval for (a) API model and, (b) New model